

# Dynamical freezing of relaxation to equilibrium

Stefano Iubini,<sup>1,2,\*</sup> Liviu Chirondoian,<sup>3</sup> Gian-Luca Oppo,<sup>3</sup> Antonio Politi,<sup>4</sup> and Paolo Politi<sup>2,5</sup>

<sup>1</sup>*Department of Physics and Astronomy, University of Padova, Via Marzolo 8, I-35131 Padova, Italy*

<sup>2</sup>*Istituto dei Sistemi Complessi, Consiglio Nazionale delle Ricerche,  
Via Madonna del Piano 10, 50019 Sesto Fiorentino, Italy*

<sup>3</sup>*SUPA and Department of Physics, University of Strathclyde, Glasgow G4 0NG, Scotland, UK*

<sup>4</sup>*Institute for Complex Systems and Mathematical Biology & SUPA University of Aberdeen, Aberdeen AB24 3UE, Scotland, UK*

<sup>5</sup>*INFN Sezione di Firenze, via G. Sansone 1, 50019 Sesto Fiorentino, Italy*

We provide evidence of an extremely slow thermalization occurring in the Discrete NonLinear Schrödinger (DNLS) model. At variance with many similar processes encountered in statistical mechanics - typically ascribed to the presence of (free) energy barriers - here the slowness has a purely dynamical origin: it is due to the presence of an adiabatic invariant, which freezes the dynamics of a tall breather. Consequently, relaxation proceeds via rare events, where energy is suddenly released towards the background. We conjecture that this exponentially slow relaxation is a key ingredient contributing to the non-ergodic behavior recently observed in the negative temperature region of the DNLS equation.

Statistical physics offers several examples of slow processes. In many cases the existence of long time scales can be traced back to the presence of (free) energy barriers, which require the emergence of strong fluctuations for them to be overcome. Structural and spin glasses, as well as colloids are strongly affected by this mechanism, [1, 2] where frustration and disorder can either give rise to aging phenomena [3] and jamming [4] or to ergodicity breaking [5], if they become insurmountable in the thermodynamic limit. Slow phenomena can however emerge also in the absence of free-energy barriers, if the onset of equipartition is slowed down due to phase-space regions characterized by a nearly integrable dynamics [6–8].

Frozen dynamics also appears in driven systems, e.g. in active matter [9] if the motion appears to be confined to a specific region, and in quantum systems [10, 11]. Another set-up which has recently attracted the interest of scientists for an unusual transport regime is a system of rotors, where the conductivity is exponentially small upon increasing the temperature [12]. This phenomenon has been shown to be related to the emergence of many-body quantum localization and ergodicity breaking. Moreover, rigorous results obtained for small rotor chains in contact with external reservoirs prove that relaxation to nonequilibrium stationary states involve stretched-exponential rates [13–15].

The Discrete NonLinear Schrödinger (DNLS) equation, the subject of this Letter, is yet another model that is frequently considered for many physical applications [16–18] and where slow phenomena may emerge as a result of intrinsic localized fast rotations usually referred to as *discrete breathers* [19–23]. This equation, which is standard to model propagation in nonlinear discrete media with negligible dissipation, is now specially used to study trapped ultra-cold gases [24–26], magnetic systems [27, 28] and arrays of optical wave-guides [29, 30]. Its fame is also due to the so-

called negative-temperature region [22, 31–33], where equipartition is violated due to the spontaneous emergence of breathers (hot spots) out of a noisy background. Statistical-mechanical arguments [34–37] show that the density of breathers should progressively decrease until a final state is reached where a single breather collects the excess energy from the background. Such relaxation process, induced by purely entropic forces, has been understood to be a condensation phenomenon [38–40] due to the existence of two conserved quantities, the mass and the energy (proportional to the square of the mass). However, the simplest condensation model [22, 41, 42] is associated to a power-law coarsening of breathers while microcanonical simulations of DNLS dynamics give evidence of a quasi-stationary regime where the number of breathers fluctuates around a well-defined average value, implying that ergodicity is broken [22, 43]. Furthermore, nonequilibrium grandcanonical simulations suggest negative-temperature regimes where high breathers do not even arise [44].

The goal of this Letter is to clarify the nature of the slow processes observed in the DNLS equation. First, we show that slow breather dynamics appears in the positive temperature regime too if we prepare the system with a tall breather sitting on a noisy background and let it relax. Second, we give evidence that relaxation is slow because an adiabatic invariant blocks diffusion, thereby leading to the effective ergodicity breaking discussed in Ref. [43].

The DNLS equation has the form

$$i\dot{z}_n = -2|z_n|^2 z_n - z_{n+1} - z_{n-1}, \quad (1)$$

where  $z_n$  are complex variables,  $n = -N_0, \dots, N_0$  is the index of the lattice site and suitable boundary conditions are assumed (see below). The model has two exactly

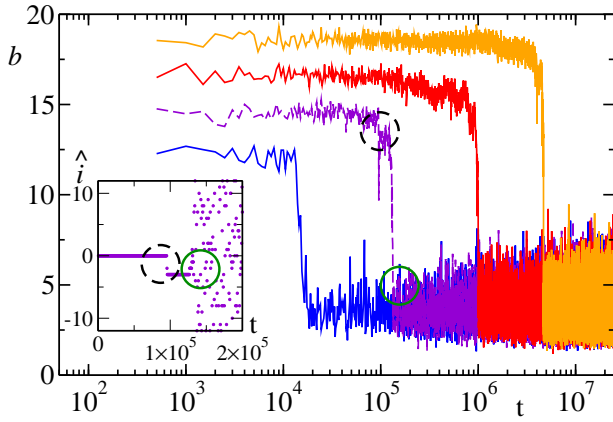


FIG. 1. Relaxation of the breather mass  $b$  on a positive temperature background for increasing initial breather heights in a DNLS chain with  $N = 31$  in contact with two thermal baths at  $T = 10$ . The inset shows the breather position  $\hat{i}(t)$  for the violet dashed line. Dashed black and full green circles identify respectively a jump and the final destruction of the breather, i.e. the onset of equipartition.

conserved quantities, namely the total energy

$$H = \sum_{n=-N_0}^{N_0} (|z_n|^4 + z_n^* z_{n+1} + z_n z_{n+1}^*), \quad (2)$$

and the total mass,  $A = \sum_n |z_n|^2$ , related to the invariance under time translation ( $t \rightarrow t + \bar{t}$ ) and phase rotation ( $z_n \rightarrow z_n e^{i\phi}$ ), respectively. If  $N = 2N_0 + 1$ ,  $h = H/N$  and  $a = A/N$  are the density of energy and mass, respectively, and the curve  $h = 2a^2$  defines the equilibrium states at infinite temperature ( $T = \infty$ ) [31].

In the DNLS (1), breathers naturally appear in the  $T < 0$  regime (defined by  $h > 2a^2$ ): their dynamics looks essentially frozen [22]. Conversely, in the  $T > 0$  regime (defined by the open region  $a^2 - 2a < h < 2a^2$  [31]), breathers are entropically disadvantaged and must decay [31, 34–37]. In this Letter we probe the positive  $T$  frozen dynamics by studying the relaxation of a single breather initially set at  $n = 0$ . Implications for the  $T < 0$  region will be discussed in the conclusions.

Breather stability has been already studied in the literature, but exclusively in the presence of a weakly fluctuating (small-amplitude) background [45]. Here, we consider a generic-amplitude background, which cannot be treated perturbatively.

Exemplary traces of the evolution of the mass  $b(t) = |z_0^2(t)|$  for a background temperature  $T = 10$  and different  $b(0)$  values are plotted in Fig. 1. There, we notice a dramatic increase of the lifetime with the initial mass (the horizontal scale is logarithmic).

The dependence of the average lifetime  $\tau_b$  on the initial mass is analyzed in a more quantitative way in Fig. 2 [46]. In each single realization,  $\tau_b$  is determined as the shortest

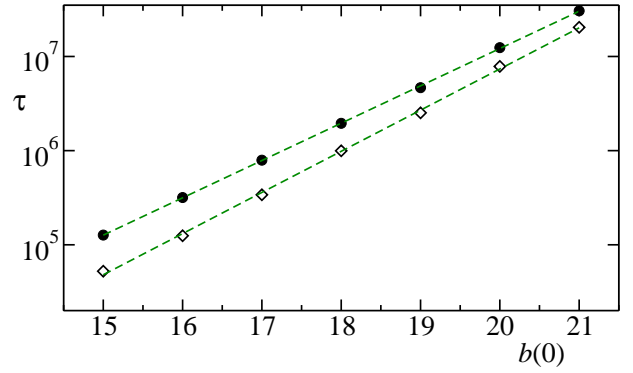


FIG. 2. Breather lifetime (black dots) and first hopping time (empty diamonds) for a chain with  $N = 31$ ,  $T = 10$  and chemical potential  $\mu = -6.4$  versus the initial breather mass  $b(0)$ . Relaxation times are computed by the first passage time, averaging over 100 realizations. Symbol sizes are of the order of the standard deviations of lifetimes.

time such that  $b(t) \leq \theta$ , where  $\theta$  is a suitable threshold. As we are interested in tall breathers ( $b(0) \gg 1$ ), and given that  $b(t)$  is characterized by a fast final drop (see Fig. 1), the choice of  $\theta$  is not a critical issue (here we have set  $\theta = 5/3$ ). We find that  $\tau_b$  increases as  $\tau_b \approx e^{\alpha b(0)}$ , with an exponent  $\alpha = 0.91 \pm 0.01$  (see black dots in Fig. 2).

In the following, we discuss the origin of this scaling behavior, starting from the empirical observation (see Fig. 1) that the mass evolution is characterized by seemingly stationary “laminar” periods [47] accompanied by a few localised episodes, where the breather amplitude decreases abruptly (though, in some cases, upward jumps are observed as well).

We start with the pseudo-stationary periods. Since they are relatively long, it makes sense to compute the correlation  $C(\tau) = \langle b(t + \tau)b(t) \rangle - \langle b(t) \rangle^2$ , where the angular brackets denote a time average (computed over an interval of order  $10^4$ ).  $C(0)$  corresponds to the variance of the fluctuations: from the data reported in Fig. 3a, we see that  $C(0)$  scales approximately as  $1/b(0)$ . The correlation exhibits rapid oscillations at the frequency of the breather for a time  $\tau \approx 1$ , before being eventually damped by the chaotic fluctuations induced by the background. This suggests that the memory of the initial condition is quickly lost. On the other hand, the two different correlation profiles obtained for the same breather mass  $b(0) = 35$  but different background configurations, reveal a dependence on the initial condition that must be understood.

In order to further clarify the behavior of  $C(\tau)$ , we have implemented the principal component analysis (PCA) [48]. We apply PCA to the configurations of a triplet composed of the breather and its two neighboring sites, i.e.  $[z_{-1}, z_0, z_1]$ . As the DNLS evolution is

invariant under a homogeneous phase shift, each triplet can be rotated until the breather variable  $z_0$  is real and positive. The resulting configuration can be thereby parametrized by five real variables,  $[u_1, u_2, u_3, u_4, u_5] \equiv [\rho_{-1} \cos \psi_{-1}, \rho_{-1} \sin \psi_{-1}, \rho_0, \rho_1 \cos \psi_1, \rho_1 \sin \psi_1]$ , where  $z_j = \rho_j e^{i\phi_j}$  and  $\psi_j = \phi_j - \phi_0$ . Given an ensemble of quintuplets, the correlation matrix  $K_{ij} = \langle u_i u_j \rangle - \langle u_i \rangle \langle u_j \rangle$ , is determined by averaging over time. The real positive eigenvalues  $\lambda_m$  of  $K_{ij}$  correspond to the variance of the underlying quasi-stationary distribution along the so-called principal axes. It turns out that while four out of the five eigenvalues are close to 1, independently of the mass  $b(0)$ , the last eigenvalue  $\lambda_{min}$  is very small and decreases upon increasing  $b$ . From the data reported in Fig. 3b, it follows that  $\lambda_{min} \approx b(0)^{-4}$ , meaning that the quasi-stationary regime unfolds within a thin flat manifold of thickness  $\xi \approx b(0)^{-2}$  (notice that  $b(0) = \rho_0^2$ ).

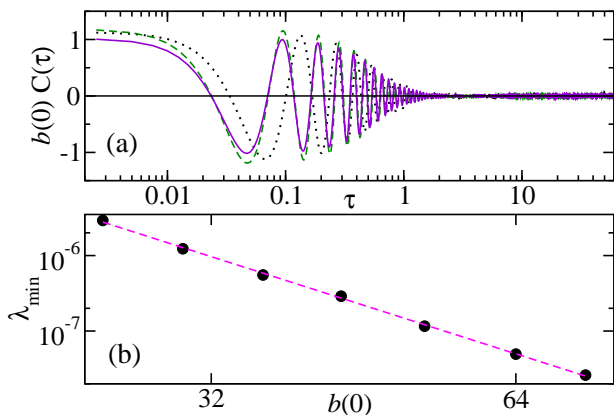


FIG. 3. (a) Correlation for different values of initial masses:  $b(0) = 25$  (black dotted curve) and  $b(0) = 35$  (violet solid and green dashed curves, for two different background realizations); (b) PCA analysis: the smallest eigenvalue of  $K_{ij}$  is plotted versus the mass  $b(0)$ .

This can be taken as evidence of a quasi-conserved quantity  $Q_1$  and explains the behavior of the correlation. In fact, while the dependence of  $C(\tau)$  on the initial condition signifies that the trajectory visits different portions of the phase space (characterized by different values of  $Q_1$ ), its decay hints at an ergodic filling of the visited region. A linear, approximate expression of the pseudo-invariant manifold can be obtained from the eigendirection corresponding to  $\lambda_{min}$ . With reference to the original variables, it writes as

$$Q_1 = \rho_0 + c[\rho_{-1} \cos \psi_{-1} + \rho_1 \cos \psi_1] \quad (3)$$

where  $c$  is a small number, which decreases upon increasing  $\rho_0$ , while the contribution of the components  $\rho_{\pm 1} \sin \psi_{\pm 1}$  is negligible.

More physical insight into  $Q_1$  can be gained using a direct perturbative derivation. The DNLS equation for

the breather amplitude can be written as  $\dot{\rho}_0 = (x_1 + x_{-1}) \sin \phi_0 - (y_1 + y_{-1}) \cos \phi_0$ , where  $\phi_0(t)$  is the phase of the breather, while  $x_{\pm 1}$  and  $y_{\pm 1}$  are the real and imaginary parts of the amplitudes  $z_{\pm 1}$ . In the tall-breather limit, we expect the existence of at least two time scales: a fast one of order  $(2\rho_0^2)^{-1}$  associated to the rotation of the breather and a slow one of order 1, associated to the background evolution. On short time scales, we can assume  $x_{\pm 1}$  and  $y_{\pm 1}$  to be constant and  $\dot{\phi}_0 = \omega \approx 2\rho_0^2$  is constant as well. Accordingly, the evolution equation for  $\rho_0$  can be integrated, yielding

$$\rho_0 = Q - [(x_1 + x_{-1}) \cos \phi_0 + (y_1 + y_{-1}) \sin \phi_0] / (2\rho_0^2), \quad (4)$$

where the integration constant  $Q$  is such only at this level of approximation.  $Q$  is a natural candidate for representing the quasi-conservation law suggested by the PCA analysis. In fact, by expressing Eq. (4) in polar coordinates, we see that it is equivalent to Eq. (3) once  $1/(2\rho_0^2)$  is identified with  $c$  and  $Q$  with  $Q_1$ . The evolution of  $Q$  superposed to that of  $\rho_0$  (see the inset of Fig. 4) provides a visual confirmation of its tiny fluctuations.

All of this suggests that we are before an adiabatic invariant (AI) and that Eq. (3) is its approximate expression. This is not entirely surprising, since AIs typically arise in the presence of a large scale separation between a relatively slow motion (here represented by the background dynamics) and rapid oscillations (here, the breather rotation). AI are a relatively standard tool in the analysis of relaxation properties at low-energy densities, where they provide a valid alternative to the Nekhoroshev formalism [49]. In the Klein-Gordon lattice, for instance, it has been proven that the destabilization time of an AI may be exponentially long in the thermodynamic limit [50]; AIs have been found also in the DNLS, but, again in the weak coupling limit [51].

In the current context, the development of an analytic treatment is hindered by the chaotic nature of the “slow” dynamics. In principle, we could derive a more accurate expression than Eq. (3) for  $Q$ , by determining higher order terms in the perturbative expansion. However, besides being a daunting task, it would be not so helpful since we anticipate that the AI stability is non-perturbative as it increases exponentially with  $\omega$ . We prefer to make use of the effective amplitude  $Q$  to investigate the diffusion of the mass of the breather. In fact, being  $Q$  characterized by much smaller fluctuations than  $\rho_0$  itself, we have better chances to find evidence of a very small diffusion. In practice, we have computed  $C_Q(\tau) = \langle [Q^2(t+\tau) - Q^2(t)]^2 \rangle$  for a time  $\tau$  long enough to see  $C_Q(\tau)$  growing linearly [52]. The results for  $D_Q = C_Q(\tau)/\tau$  are plotted in Fig. 4 [46], where the diffusion coefficient is shown to decrease exponentially with the breather mass,  $D_Q \approx e^{-\gamma b(0)}$ , with  $\gamma = 1.13 \pm 0.09$ .

During the laminar periods, the background is basically at equilibrium with a temperature and a chemical

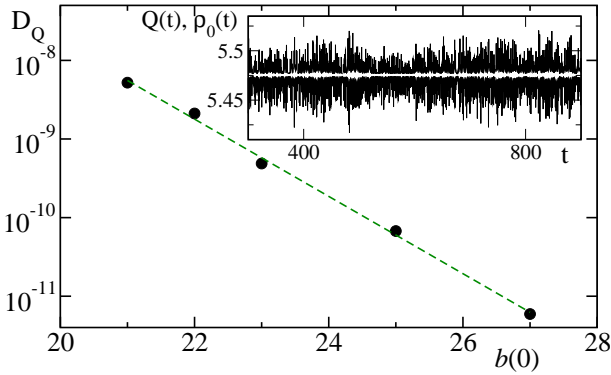


FIG. 4. Diffusion coefficient  $D_Q$  as a function of the initial breather mass. The inset shows the evolution of  $Q(t)$  (white line) compared to that of the breather amplitude  $\rho_0(t)$  (black line).

potential self-adjusted according to the setting of the external reservoir. Accordingly, the background itself can be interpreted as an effective thermal bath, which interacts directly with the breather. Fluctuation-dissipation considerations then suggest that the interaction should be characterized by a diffusion coefficient that can be identified with the above defined  $D_Q$ , and a drift  $v$ , responsible for the eventual absorption of the breather. In fact, for  $T > 0$  the equilibrium state of the DNLS is statistically homogeneous, with no breathers. According to the same fluctuation-dissipation considerations,  $v$  is expected to be proportional to  $D_Q/T$ , as also confirmed by explicit calculations for a simple model [42]. As a result, in the absence of jumps, we expect that the lifetime of the breather should be at least of the order of  $b(0)/v \approx b(0)e^{\gamma b(0)}$ . Notice that  $\gamma$  is slightly larger than the direct estimate  $\alpha$ . We can at least conclude that the laminar phase dynamics is compatible with the exponential growth of the breather lifetime [53].

We finally come back to the sporadic jumps that delimit laminar periods. Preliminary simulations show that they are triggered by anomalously large fluctuations of the background. In order to quantify the phenomenon, we have computed  $\Delta\epsilon = \langle |\Delta b^2| \rangle$ , where  $b^2(t)$  is the breather energy, while  $\Delta\epsilon$  indicates its variation after 50 time units [46]. The breather, of initial mass  $a_1 = b(0) = 36$ , is set on one boundary of the chain ( $N = 9$ ) [46]; the neighbouring site has an initial mass  $a_2 = rb(0)$ , while the opposite boundary is thermalized at  $T = 10, \mu = -6.4$ . A plot of the breather energy variation as a function of  $r$ , see Fig. 5, clearly shows a peak at  $r_d = (\sqrt{b(0)} - \sqrt{2})^2/b(0)$  (see the vertical line); it corresponds to the threshold for the formation of a symmetric dimer state [54]. Since a dimer, once excited, can relax back to a breather sitting on either site, its onset is associated to breather hopping, a phenomenon that is indeed observed in numerical simulations (see, e.g., the

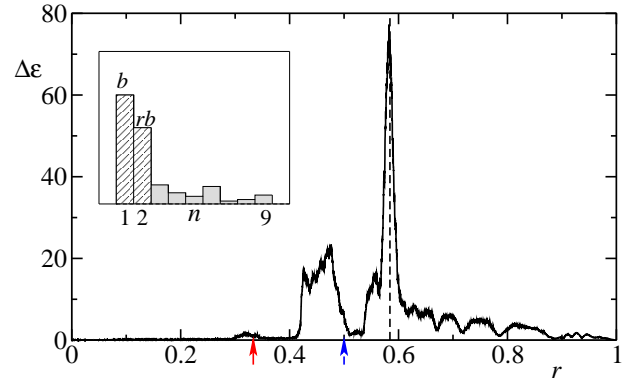


FIG. 5. Average jumps of breather energy,  $\Delta\epsilon$ , as a function of the mass ratio  $r$ . The inset depicts the geometry of the system. The highest peak corresponds to the analytical value  $r_d$  (dashed line). The resonance values  $r_3$  and  $r_2$  are indicated by the arrows.

inset of Fig. 1). As shown in Fig. 2, the average first hopping time  $\tau_h$  (open diamonds) increases exponentially with  $b(0)$  (with a rate  $\alpha_h = 1.00 \pm 0.04$ ), revealing that jumps too contribute to exponentially-long breather lifetimes.

A semi-quantitative estimate of  $\tau_h$  can be obtained by approximating it with the (average) time  $\tau_\theta$  required for a background fluctuation to reach the threshold  $\theta = r_d b$ ;  $\tau_\theta$  roughly corresponds to the inverse of the probability  $P(\theta)$  to observe the mass  $\theta$  at equilibrium. From [31], we know that for large temperature  $T = 1/\beta$ ,  $P(\theta) = \sqrt{4\beta/\pi} e^{-\beta(\theta^2 - \mu\theta + \mu^2/4)} / [1 + \text{erf}(\mu\sqrt{\beta}/2)]$ , where  $\mu$  is the chemical potential. In the limit of large  $b$ ,  $\tau_\theta \approx \exp(r_d^2 \beta b^2)$ , i.e. this rough argument suggests that first-hopping time might even grow super-exponentially with  $b$ . Unfortunately, this prediction is not fully quantitative, as the probability density in the breather nearest neighbours is affected by the breather itself and is only approximately equal to the equilibrium distribution.

All of our studies consistently give evidence of an exponentially slow relaxational dynamics. The origin of such freezing process is very different from the arrest mechanisms typically encountered in statistical mechanics: it has a purely dynamical origin, being enforced by the existence of an adiabatic invariant (AI). For  $T > 0$ , the AI neutralizes entropic forces, preventing *de facto* a macroscopic relaxation as soon as a few tall breathers are contained in the initial configuration. Indeed, in the presence of an exponentially weak effective breather-background interaction, breather condensation proceeds through a practically unobservable logarithmic coarsening [42]. In the negative-temperature region, the same mechanism prevents breather growth, thereby “stabilizing” a fairly homogeneous chaotic non-ergodic dynamics, as suggested by recent direct numerical simulations [22, 43].

Finally, we point to the major open problem: whether



the simultaneous slowness of the diffusion and of the jumps is a mere coincidence, or the indication of a deeper relationship. By looking back at Fig. 5, one can see additional peaks besides  $r_d$ , which approximately coincide with resonances, where the frequency on the first site is equal to  $1/3$  ( $r_3$ ) and  $1/2$  ( $r_2$ ) of the breather frequency. Such resonances too contribute to the decay of the breather and, although the single events are less effective, they are much more frequent than the dimer formation. Could it be that the diffusion which characterizes laminar periods is nothing but a collection of jumps of different sizes associated to different resonances? The answer to this question necessarily passes through a more accurate characterization of the adiabatic invariant.

We thank S. Lepri and R. Livi for a critical reading of the manuscript. S.I. acknowledges support from Progetto di Ricerca Dipartimentale BIRD173122/17.

---

\* stefano.iubini@unipd.it

- [1] L. Berthier and G. Biroli, *Rev. Mod. Phys.* **83**, 587 (2011).
- [2] L. Cipelletti and L. Ramos, *Journal of Physics: Condensed Matter* **17**, R253 (2005).
- [3] L. F. Cugliandolo, “Dynamics of glassy systems,” (2002), arXiv:cond-mat/0210312.
- [4] V. Trappe, V. Prasad, L. Cipelletti, P. Segre, and D. A. Weitz, *Nature* **411**, 772 (2001).
- [5] R. Palmer, *Advances in Physics* **31**, 669 (1982).
- [6] E. Fermi, P. Pasta, S. Ulam, and M. Tsingou, *Studies of the nonlinear problems*, Tech. Rep. (Los Alamos Scientific Lab., N. Mex., 1955).
- [7] G. Berman and F. Izrailev, *CHAOS* **15**, 015104 (2005).
- [8] G. Gallavotti, *The Fermi-Pasta-Ulam problem: a status report*, Vol. 728 (Springer, 2007).
- [9] C. Reichhardt and C. J. O. Reichhardt, *Proceedings of the National Academy of Sciences* **108**, 19099 (2011).
- [10] B. N. Balz and P. Reimann, *Physical review letters* **118**, 190601 (2017).
- [11] Z. Lan, M. van Horssen, S. Powell, and J. P. Garrahan, *Physical review letters* **121**, 040603 (2018).
- [12] M. Pino, L. B. Ioffe, and B. L. Altshuler, *Proceedings of the National Academy of Sciences* **113**, 536 (2016).
- [13] N. Cuneo, J.-P. Eckmann, and C. Poquet, *Nonlinearity* **28**, 2397 (2015).
- [14] N. Cuneo and J.-P. Eckmann, *Comm. Math. Phys.* **345**, 185 (2016).
- [15] N. Cuneo, C. Poquet, *et al.*, *Electronic Communications in Probability* **22** (2017).
- [16] T. Holstein, *Annals of Physics* **8**, 325 (1959).
- [17] J. Eilbeck, P. Lomdahl, and A. Scott, *Physica D* **16**, 318 (1985).
- [18] P. G. Kevrekidis, *The Discrete Nonlinear Schrödinger Equation* (Springer Verlag, Berlin, 2009).
- [19] C. Eilbeck and M. Johansson, in *Localization and energy transfer in nonlinear systems* (World Scientific, 2003) pp. 44–67.
- [20] G. Ng, H. Hennig, R. Fleischmann, T. Kottos, and T. Geisel, *New Journal of Physics* **11**, 073045 (2009).
- [21] R. Franzosi, R. Livi, G. Oppo, and A. Politi, *Nonlinearity* **24**, R89 (2011).
- [22] S. Iubini, R. Franzosi, R. Livi, G.-L. Oppo, and A. Politi, *New Journal of Physics* **15**, 023032 (2013).
- [23] J.-P. Eckmann and C. E. Wayne, arXiv preprint arXiv:1710.10999 (2017).
- [24] A. Trombettoni and A. Smerzi, *Phys. Rev. Lett.* **86**, 2353 (2001).
- [25] R. Livi, R. Franzosi, and G.-L. Oppo, *Phys. Rev. Lett.* **97**, 060401 (2006).
- [26] H. Hennig, J. Dorignac, and D. K. Campbell, *Phys. Rev. A* **82**, 053604 (2010).
- [27] S. Borlenghi, W. Wang, H. Fangohr, L. Bergqvist, and A. Delin, *Phys. Rev. Lett.* **112**, 047203 (2014).
- [28] S. Borlenghi, S. Iubini, S. Lepri, J. Chico, L. Bergqvist, A. Delin, and J. Fransson, *Phys. Rev. E* **92**, 012116 (2015).
- [29] S. Jensen, *Quantum Electronics, IEEE Journal of* **18**, 1580 (1982).
- [30] D. Christodoulides and R. Joseph, *Optics Letters* **13**, 794 (1988).
- [31] K. Rasmussen, T. Cretegny, P. Kevrekidis, and N. Grønbech-Jensen, *Phys. Rev. Lett.* **84**, 3740 (2000).
- [32] U. Levy and Y. Silberberg, *Phys. Rev. B* **98**, 060303 (2018).
- [33] A. Y. Cherny, T. Engl, and S. Flach, arXiv preprint arXiv:1809.05371 (2018).
- [34] B. Rumpf, *Phys. Rev. E* **69**, 016618 (2004).
- [35] B. Rumpf, *EPL (Europhysics Letters)* **78**, 26001 (2007).
- [36] B. Rumpf, *Physical Review E* **77**, 036606 (2008).
- [37] B. Rumpf, *Physica D: Nonlinear Phenomena* **238**, 2067 (2009).
- [38] J. Szavits-Nossan, M. R. Evans, and S. N. Majumdar, *Phys. Rev. Lett.* **112**, 020602 (2014).
- [39] J. Szavits-Nossan, M. R. Evans, and S. N. Majumdar, *J. Phys. A: Mathematical and Theoretical* **47**, 455004 (2014).
- [40] J. Barré and L. Mangeolle, *Journal of Statistical Mechanics: Theory and Experiment* **2018**, 043211 (2018).
- [41] S. Iubini, A. Politi, and P. Politi, *Journal of Statistical Physics* **154**, 1057 (2014).
- [42] S. Iubini, A. Politi, and P. Politi, *Journal of Statistical Mechanics: Theory and Experiment* **2017**, 073201 (2017).
- [43] T. Mithun, Y. Kati, C. Danieli, and S. Flach, *Phys. Rev. Lett.* **120**, 184101 (2018).
- [44] S. Iubini, S. Lepri, R. Livi, G.-L. Oppo, and A. Politi, *Entropy* **19**, 445 (2017).
- [45] M. Johansson and K. Ø. Rasmussen, *Phys. Rev. E* **70**, 066610 (2004).
- [46] For the technical details of the simulations see the Supplementary Material.
- [47] The increasing size of the fluctuations is a deceptive effect due to the horizontal logarithmic scale, which compresses an increasing number of points in the same interval at longer times.
- [48] I. Jolliffe, *Principal component analysis* (Springer Series in Statistics, Springer-Verlag, New York Berlin Heidelberg, 2002).
- [49] M. Guzzo, “An overview on the nekhoroshev theorem,” in *Topics in Gravitational Dynamics: Solar, Extra-Solar and Galactic Systems*, edited by D. Benest, C. Froeschle, and E. Lega (Springer, Berlin, 2007) pp. 1–28.
- [50] A. Carati and A. M. Maiocchi, *Communications in Mathematical Physics* **314**, 129 (2012).
- [51] A. Giorgilli, S. Paleari, and T. Penati, *J. Stat. Phys.* **148**, 1106 (2012).

- [52] The reason of the inner square in the definition of  $C_Q$  is that we are interested in a mass-like variable such as  $Q^2$ .  
 [53] We have not been able to estimate directly  $v$ , presumably since it is smaller than  $D_Q$ , because of the  $1/T$  multiplica-

- tive factor.  
 [54] V. M. Kenkre and D. K. Campbell, Phys. Rev. B **34**, 4959 (1986).

## Details of computational analysis

*Numerical evolution of the DNLS dynamics in the presence of energy and mass reservoirs* - Given the need to run long simulations, we defined an optimal set-up to minimize the computation time. As a reference setup, we have chosen to simulate DNLS chains of length  $2N_0 + 1$  with a breather sitting in the middle and both chain ends attached to suitable heat baths (see below).

It is desirable to choose  $N_0$  as short as possible, but not too short otherwise the overall scenario is strongly affected by boundary layers which emerge in the vicinity of the heat baths. We have verified that for  $N_0 \geq 9$  such effects are negligible and the lifetime is independent of  $N_0$ . Two different integration schemes have been implemented:

- (i) Langevin-type thermal baths [1] together with a standard fourth-order Runge-Kutta algorithm [2] (and a sufficiently small integration time step even down to  $10^{-5}$  time units so as to follow the fast rotation of the breather);
- (ii) Monte Carlo thermal baths [3] with a symplectic fourth-order Yoshida algorithm [4] (minimum time-step  $10^{-3}$  time units).

For scheme (i), the explicit Langevin equation (specified for the last lattice site) reads

$$i\dot{z}_{N_0} = (1 + i\Gamma) [-2|z_{N_0}|^2 z_{N_0} - z_{N_0+1} - z_{N_0-1}] + i\Gamma\mu z_{N_0} + \sqrt{\Gamma T}\eta(t) \quad , \quad (5)$$

where  $\eta(t)$  is a complex Gaussian white noise with zero mean and unit variance and  $\Gamma$  is the bath coupling parameter. Without any loss of generality, we have chosen  $\Gamma = 1$ .

For scheme (ii), according to [3], the two Monte Carlo reservoirs interact with the DNLS chain at random times whose separations are independent and distributed uniformly within the interval  $[t_{\min}, t_{\max}]$ . We have chosen  $t_{\min} = 0.4$  and  $t_{\max} = 2$ . We have verified that the two numerical approaches are consistent with each other.

*Figure 4* - The results for the diffusion coefficient have been obtained by scanning the entire breather evolution and discarding all the time intervals where the mass of either neighbor site is larger than 8, to exclude the occasional jumps caused by sudden increase of the amplitude in the neighboring sites.

*Figure 5* - The slightly different setup with the breather placed on one boundary of the DNLS chain is chosen in order to cleanly study the effect of just one neighboring background site with an anomalously large mass fluctuation. The results shown in Fig. 5 refer to an ensemble of initial conditions where the phase difference  $\phi_2 - \phi_1$  is set to  $\pi$ , because results not shown in the Letter prove that it is the condition to ensure the best coupling with the breather.

---

\* stefano.iubini@unipd.it

- [1] S. Iubini, S. Lepri, R. Livi, and A. Politi, Journal of Statistical Mechanics: Theory and Experiment **2013**, P08017 (2013).
- [2] W. H. Press, S. A. Teukolsky, W. T. Vetterling, and B. P. Flannery, *Numerical recipes 3rd edition: The art of scientific computing* (Cambridge university press, 2007).
- [3] S. Iubini, S. Lepri, and A. Politi, Physical Review E **86**, 011108 (2012).
- [4] H. Yoshida, Physics Letters A **150**, 262 (1990).